Eng. & Technology, Vol.25, No.7, 2007

Cumulative Damage in Fatigue of a Structure Subjected to Random Loading

Dr.Kadhim Karim Muhsin*

Received on: 25/1/2006
Accepted on: 20/5/2007

Abstract

When a structure is subjected to a random loading, its dynamic response changes, characterized by shifts in the eigenvalues and modification of eigenvectors. The peaks in the dynamic response spectrum will give indications of the natural frequencies of the structure. Any damage in the structure will be reflected in the spectrum as a shift in natural frequencies.

Crack initiation and early growth of fatigue cracks in 0.4% carbon steel and 2024-T4 aluminum are investigated using spectral density approach for applied random loading. Energetic consideration and spectral density approach lead to the formulation of a model used to predict the behavior of short and long cracks initiation, propagation, and paths taking into account the microstructural variables relevant to fatigue crack initiation and early crack growth.

The model indicates that crack arrest occurs when crack-tip is blocked by a grain boundary. In the short crack region, propagation and non-propagation occurs depending on random loading stress level and slip band energy released. The application of the present model to cumulative damage is compared with the experimental data and a reasonable agreement is found. The introduction of material specification shows a quantitative description of the parameters which affect the reliability of a structural component subjected to random loading. The power of the analytic model and the simulation analysis in the present work give some insight to the behavior of the structure under random loading showing the different mode shapes, eigenvalues/vectors, deformation, propagation and non-propagation of cracks, and the stresses caused by such random loading that can lead to fatigue failure. A life predication model is presented for long-life fatigue , to control the hardware design and to find a proper combination of random load and life .

تراكم الضرر في الهياكل المعرضة لأحمال عشوائية

الخلاصة

تتغير الاستجابة الديناميكية للهياكل المعرضة لأحمال عشوائية ويتمثل ذلك في الانحراف في الترددات الطبيعية وتعديلات في النسوق. القمم ي الاستجابة الديناميكية الطيفية تعطي إشارة عن الترددات الطبيعية لهياكل. وأن أي ضرر في الهيكل سوف ينعكس في الكثافة الطيفية كانحراف في الترددات الطبيعية. تم دراسة نشوء الشق والنمو المبكر لشقوق الكلل لعينات ٠,٤ % فولاذ كار بوني و 2024-T4 ألمنيوم باستخدام طريقة الكثافة الطيفية المعرضة لحمل عشوائي ، من خلال اعتبارات الطاقة وطريقة الكثافة الطيفية ، تم بناء نموذج رياضي يتنبأ بتصرف الشقوق القصيرة والطويلة ونشوء الشق والنمو ومساره مع الأخذ بنظر الاعتبار المتغيرات المجهرية المتعلقة بنشوء ونمو الشق.النموذج الرياضي يوضح بأن الشق يتوقف عندما يصطدم بالحدود الحبيبية بينما في منطقة الشق القصير يحدث النمو وعدم النمو للشق اعتماداً على مستوى اجهاد الحمل العشوائي وتحرر طاقة حزم الجزيئة الانزلاقية . إن تطبيق النموذج الحالي للضرر المتراكم تم مقارنته مع النتائج العملية التي تم إيجادها ، والمقدمة وضحت الوصف النوعي للمعاليم التي تؤثر على الوثوقية في مكونة الهيكل ، كذلك فسرت عملية تحليل النموذج و المحاكاة سلوك الهيكل المعرض لحمل عشوائي لمختلف النسوق إضافة إلى الترددات والتشوه ونمو الشق وعدم النمو للشق والاجهاد الناتج عن الحمل العشوائي المسبب للفشل . كذلك تضمن البحث بناء نموذج

* Ph.D in Mechanical Eng., Applied Mechanics, University of Basrah

http s://doi.org/10.30684/etj.25.7.8
2412-0758/University of Technology-Iraq, Baghdad, Iraq

رياضي يصف عمر الكلل الطويل لغرض السيطرة على عمليات التصميم لتحديد الربط المناسب بين العمر والحمل العشوائي.

Nomenclature

A (mm^2)	= cross-sectional area
a (μm)	= crack length
ai,ac (μm)	= initial and critical crack length
b	= burger vector
C_i (N.s/mm)	= damping coefficients
D (mm)	= grain diameter
E (Gpa)	= young's modulus
E[ ]	= expectation operator
F	= geometrical calibration function
Fi (Hz)	= modal frequency
G ($N/ mm^2/c$)	= energy release rate
$H_{jk}(\omega)$	= complex frequency response
I (mm^4)	= area moment of inertia
K (N/mm)	= stiffness matrix
L (mm)	= beam length
Mi (kg)	= mass matrix
n	= constant
$Ry(\tau),Rp(\tau)$	= output and input autocorrelation function
$Sy(\tau),Sp(\omega)$ (N^2/Hz)	= output and input spectral density
So (N^2/Hz)	= white noise spectrum
μ	= shear modulus
ξi	= damping ratios
Ψij	= modal matrix
σ^2_s (N^2/ mm^4)	= variance of the random stress
σ_s (N/ mm^2)	= standared devation of the random stress
ωi (rad/sec)	= eigenvalues
ρ (kg/mm^2)	= material density
ϕ	= crystallographic function
DOF	= degree of freedom

Introduction

The dynamic response of structures to random loading has been a subject of great interest to design engineers who are responsible for the geometry of the design as well as maintenance, and material engineers who are responsible for the selection of material and manufacturing routes. This interest is primarily motivated by a desire to improve structure quality, to increase the life of components , to prevent loading damage, and most of all to ensure safe operation with increased loading and operation at higher speeds. It is very desirable to improve the performance of the components and their reliability [1].
Since the structure is subjected to random, loading, a statistical representation of these loads is required . A mathematical model of varying complexity has been developed to analyze the dynamic behaviuor of structure in response to random loads, Fourier series methods of solution have been employed. Linear analytical tools such as eigen values/vectors and transfer function can be used for preliminary design and evaluation of structure performance. Spectral and auto correlation analysis techniques can be employed for a linearized structure model to determine the random characteristics of structure (elongation, dynamic loads, stress). Items of interest include the peak values, RMS values, probability of exceeding a particular level or range, dominating frequencies, and further study of cumulative damage of components[2].

Energetic consideration often yields correct qualitative results. Digital simulation can overcome this difficulty and can handle these random effects. However, this technique is suitable as a design tool since it is less costly and the results are easy to interpret [3].

Designers need to interpret structure response in familiar terms, i.e. natural frequencies, damping ratios and modes of vibration. The present work examines the cumulative damage under random loading through analytical and experimental study. The structure responses to random loading are studied using spectral density and auto correlation approach.

Experimental Details

Instruments Used for The Experiments

Fig. (1) illustrates the instruments used for the present work. The dual channel signal analyzer type 2032 is used to analyze the beams responses, auto and cross spectra, auto and cross correlation, probability density and distribution, This signal analyzer is flexible, easy to use and fully self contained two channel FFT analysis system with 801 lines of resolution.

The power amplifier type 2707 drives the exciter body to full rating and is a powerful variable frequency source in combination with frequency generator.

The vibration exciter type 4810 introduces forced vibration in the beam and it is environmental testing of structures and used for fatigue testing of specimens, resonance searching, and for the study of dynamic properties of beams models. The force transducer type 8200 measures the dynamic, short duration static and impact force of beams, the frequency response

function, and the dynamic displacement of the beam surface.

The charge amplifier type 2635 is used for field and laboratory measurement of vibration in terms of acceleration, velocity, and displacement together with piezoelectric accelerometer and voltmeter or measuring amplifier.

Material [2]

Two types of materials were tested during the course of this work. The first is a normalized medium carbon steel containing following chemical composition (wt%) 0.4C;0.1Si;0.01S;0.005P;1.0Mn; balance Fe, and the mechanical properties are; yield stress(σ_y=282 N/mm^2), ultimate strength (σ_y=557 N/mm^2), modulus of elasticity (E=200Gpa) and reduction in area (R.A=36%).

The second material is an aluminum alloy (Al 2024-T4) consisting of the following chemical composition (wt %) 0.053 Zn; 1.51 Mg; 4.21 C; 0.347 Fe ; 0.07 Cr; 0.344 Si; 0.983 Mn; 0.027Ni; 0.015Pb; o.oo1Cd; 0.031 Sn; 0.02Ga, and the mechanical properties are yield stress (σ_y=376 N/mm^2) , ultimate strength (σ_y=501 N/mm^2) , modulus of elasticity (E=73 Gpa), and reduction in area (R.A=13%).The average grain size on the transverse plane to the beam axis was 40-50 μm.

Specimen geometry

Fig.(2) shows the standard specimen dimensions which can be used as a simply-supported beam (S.S.B) or cantilever and then is subjected to ergodic stationary gaussian random loading by the vibration exciter at room temperature to examine the behavior of short crack, initiation, propagation, non-propagation, paths , and failure.

Measurement of crack length

Fig.(3) illustrates the D.C Potential drop technique used to measure the crack length,essentially a large constant current (~30 amps) is passed through the specimen . As the crack grows the potential field in the specimen is distributed and this disturbance is detected by a pair of potential probes ,usually spot-welded on either side of the crack mouth. The bulk of the signal is "backed off " by the voltage source so that small changes in crack length can be detected.As the measured voltage is generally of the order of microvolts (steel and titanium) or nanovolts (aluminum) ,sensitive and stable amplifier and voltage sources are required ,a constant temperature environment is also desirable. If adequate precautions are taken, apparent increase in crack length 10^{-9} mm can be detected in some materials.

Cumulative Damage Under Random Loading: *A Model*

A model design to describe the crack growth under random loading (see Fig.٤) should take into account the crystallographic nature of early crack growth, the location in the metal structure where cracks develop, their path, the obstacles that they must surmount to become dominant, spectral density of the applied random loads, damping ratios and natural frequencies. Summarizing the metallographic evidence presented earlier, we notice a crack initiates in the soft slip bands probably at the grain boundary. It then propagates right across the grain until it reaches an obstacle, where depending on its strength, the crack is arrested or only temporarily halted [4].The microprocesses of crack

growth need to be related to the energy consideration of crack extension. The rate of energy released in a cycle by the structure, in order to extend the crack a distance da, is the energy release rate and it follows that

$$G = dU/dR \quad (1)$$

where U is the energy of the slip band and dU/dR is the rate of change of slip band energy with slip band length. During one cycle the slip band associated with the crack can be simulated to a linear distribution of close packed dislocations [5,6].

The energy of this type of distribution of dislocation is given by [6]:

$$U = \frac{1}{2}\int_{ro}^{R} \frac{m\,(nb)^2}{r}\,dr \quad (2)$$

where μ is the shear modulus, n is the number of dislocation in the slip band, b is the Burger vector , r_o is the core radius of the first dislocation, R is the slip band length and r is a variable length in front of the crack and along the slip band.

Integrating equation(2) where r is the only variable:

$$U = \frac{m\,(nb)^2}{2}\ln\left[\frac{R}{r_o}\right] \quad (3)$$

As the crack length *a* increases , R decreases, therefore the change of the energy of the systems with *a* may be equated to the change of the slip band energy with R and following the Griffith approach

$$\frac{dU}{dR} = \frac{m(nb)^2}{2R} = G = \frac{S^2}{m}pa$$

$$\mathrm{nb} = (2paR)^{1/2}\,\frac{S}{m} \quad (4)$$

where S = Random stress. By taking the crack extension per cycle to be proportional to the displacement along the slip band

$$\frac{da}{dN} = f\,(2paR)^{1/2}\,\frac{S}{m} \quad (5)$$

where *f* is a function of the geometry of the component which is the fraction of the dislocations on the slip which takes part in the process of crack extension. The value of R(the effective slip band length) depends on the distance and strength of the next barrier which in turn depends on the ratio of the random stress of the two grains separated by the barrier.

The argument used by Chan and Lankford [4] to define the change in crack tip plastic zone can be modified here as,

$$R = D\left[1 - f\left(\frac{D-2x}{D}\right)^n\right] \quad (6)$$

where D is the grain diameter and ϕ is the crystallgraphic orientation of the adjacent grain; grain A where the crack develops and grain B in which the crack will next propagate. In terms of the resolved random stress, the function ϕ is expressed as follows:-

$$f = 1 - \frac{S_B}{S_A} \quad (7)$$

The ratio S_B/S_A is used as a measure of the propensity of propagation of slip onto the neighboring grain , the initiation in grain *B* occurs when $S_B > S_A$. The maximum value of ϕ is unity and represents the case where the slip orientation of the next grain is most unfavorable and the crack will arrest. The case of high stress occurs when the value of ϕ is zero where the random stress is $S_B = S_A$. The value of *x* is the distance from crack-tip to the nearest grain boundary on the plane of the crack ($0 < x < D$).

By substituting Eq.(6) in Eq. (5) we obtain

$$\frac{da}{dN} = f(2paD)^{1/2}[1-f(\frac{D-2x}{D})^{n}]^{1/2}\frac{s}{m}S \quad (8)$$

The crack growth rate is itself a random variable. The average crack growth rate E[da/dN] then becomes

$$E[\frac{da}{dN}] = f(2paD)^{1/2}[1-f(\frac{D-2x}{D})^{n}]^{1/2}\frac{s}{m}S \quad (9)$$

where σ_s is the standard deviation of random stress (RMS).

Spectral density approach

The uncoupled linear equation of motion of a structure subjected to stationary ergodic random loading p(t) having Gaussian distribution and Rayliegh peaks[7,8] (see Fig.5,6) can be written in the form [7].

$$M\ddot{y}+C\dot{y}+ky=P(t) \quad (10)$$

where (*M, C, K*) represent the mass, damping, and stiffness matrices of the structure respectively.

The complex frequency response is obtained by making the substitution:

$$y(t) = \int_{-\infty}^{\infty} Y(iw)EXP(iwt)dw$$

$$p(t) = \int_{-\infty}^{\infty} P(iw)EXP(iwt)dw$$

$$\dot{y}(t) = \int_{-\infty}^{\infty} iwY(iw)EXP(iwt)dw$$

$$\ddot{y}(t) = \int_{-\infty}^{\infty} -w^2Y(iw)EXP(iwt)dw$$

In equation (10) and canceling the exp(iω) terms we obtain the receptance as:-

$$H(iw) = [k - w^2M + iwc]^{-1} \quad (11)$$

The square modulus of the complex frequency response is:-

$$|H(w)|^2 = \frac{1}{k^2[(1-w^2/w_n^2)^2 + (2zw/wn)^2]} \quad (12)$$

Mean value of the response (displacement)

From the definition of autocorrelation [9]

$$Ry(t) = \lim_{t\to\infty}\frac{1}{2T}\int_{-T}^{T} y_j(t)y_j(t+t)dt \quad (13)$$

From the impulse response function (see equation A2 in the appendix)

$$y_j(t) = \int_0^{\infty} P_j(t-t_1)h_{j_k}(t_1)dt_1 \quad (14)$$

The integer j can take values between 1 and m, where m is the number of degree of freedom , and h_{jk} is the response function for a unit impulse. Similarly

$$y_j(t+t) = \int_0^{\infty} p_j(t+t-t_2)h_{jk}(t_2)dt_2 \quad (15)$$

Substituting Eqs.(14) and (15) in Eq.(13) and rearranging the order of integration gives

$$Ry(t) = \int_0^{\infty} h_{ik}(t1)\int_0^{\infty} h_{jk}(t_2)\lim_{t\to\infty}\frac{1}{2T}x$$

$$\int_{-T}^{T} P_j(t-t_1)P_j(t+t-t_2)dtdt_2dt_1 \quad (16)$$

But

$$Rp(t+t-t_2) = \lim_{T\to\infty}\frac{1}{2T}$$

$$\int_{-T}^{T} Pj(t-t_1)Pj(t+t-t_2)dt \quad (17)$$

Then

$$Ry(t) = \int_0^{\infty} h_{jk}(t_1)\int_0^{\infty} h_{jk}(t_2)$$

$$Rp(t - t_2 + t_1)dt_2 dt_1 \quad (18)$$

From Winer-Khintchine relation [10] or the Fourier pair (see equation A3-A6 in the appendix)

$$\left.\begin{aligned} Ry(t) &= \frac{1}{4p}\int_{-\infty}^{\infty} y(w)Exp(iwt)dw \quad (a)\\ Sy(w) &= 2\int_{-\infty}^{\infty} Ry(t)Exp(iwt)dw \quad (b) \end{aligned}\right\} \quad (19)$$

where S_y (ω) is the spectral density of the responses. Substituting from Eq. (18) in the second term of fourier pair relation

$$Sy(w) = \int_{-\infty}^{\infty} Exp(-iwt)\int_{0}^{\infty} h_{jk}(t_1)$$

$$\int_{-\infty}^{\infty} h_{jk}(t_2)R_P(t - t_2 - t_1)\ dtdt_2 dt_1 \quad (20)$$

After some arrangements and multiplying by Exp(iωτ1), Exp(iωτ2), Exp[-iω (τ+τ1-τ2)] where their product is unity

$$S_y(w) = 2\int_{-\infty}^{\infty} hjk(t_1)Exp(iwt_1)\int_{-\infty}^{\infty} hjk(t_2)Exp(-iwt_2)$$

$$\times \int_{-\infty}^{\infty} R_P(t - t_2 + t_1)Exp[-iw(t + t_1 - t_2)dtdt_2 dt_1$$

$$= \int_{-\infty}^{\infty} h_{jk}(t_1)Exp(iwt_1)\int_{-\infty}^{\infty} h_{jk}(t_2)Exp(-iwt_1)$$

$$\times 2\int_{-\infty}^{\infty} Rp(t_3)Exp(-iwt_3)(dtdt_2 dt_1 \quad (21)$$

where $\tau_3 = \tau - \tau_2 + \tau_1$

$Sy(\omega) = I_1 + I_2 + I_3$

$I_1 = H_{jk}(\omega)$, $I_2 = H_{jk}(-\omega)$, $I_3 = Sp_j(\omega)$

where H_{jk} (-ω) is the matrix conjugate transposition

Thus

$$Sy_j(w) = \left|H_{jk}(w)\right|^2 Spj(w) \quad (22)$$

From the first term of Fourier pair we obtain

$$R(0) = E\left[y_j^2(t)\right] = \frac{1}{4p}\int_{-\infty}^{\infty} Sy_j(w)dw = \frac{1}{2p}$$

$$\int_{0}^{\infty} Sy_j(w)dw \quad (23)$$

Substituting equation (22) in equation (23) we obtain

$$E\left[y_j^2(t)\right] = \frac{1}{2p}\int_{-\infty}^{\infty}\left|Hjk(w)\right|^2 Spj(w) \quad (24)$$

Random Loading Spectral densities Sp(ω)

For white noise Gaussian random loading Sp(ω) = So shown in Fig.7 (a), the mean response (displacement) is found from equation (12) and equation (24) as

$$E\left[y^2(t)\right] =$$

$$\frac{1}{2p}\int_{0}^{\infty}\frac{So}{k^2\left[(1 - w^2/w_n^2)^2 + (2xw/w_n)^2\right]}dw \quad (25)$$

Integrating equation (25) by the calculus of residues gives

$$E\left[y^2(t)\right] = \frac{So\,w_n}{8xk^2} \quad (26)$$

For Band-Limited Gaussian random loading in Fig. 7(b), the spectral density Sp(ω) is uniform up to a cut-off frequency, which is well above the natural frequency

The mean value is found as

$$E\left[y^2(t)\right] =$$

$$\frac{1}{2p}\int_{0}^{wc}\frac{So}{k^2\left[(1 - w^2/w_n^2)^2 + (2xw)^2\right]}dw \quad (27)$$

$$E\left[y^2(t)\right] \approx \frac{Sow_n}{8xk^2} \quad (28)$$

For slow Gaussian random loading in Fig. 7(c), the spectral density Sp(ω)varies fairly slowly with ω according to the curve $Sp(\omega)=S_o-S_2(\omega/\omega_n)$.
Then the mean value is ,

$$E\left[y^2(t)\right]=\frac{Sp(w)w_n}{8xk^2}$$

$$E\left[y^2(t)\right]=\frac{(S_o-S_2)w_n}{8xk^2} \qquad (29)$$

Standard deviation of random stress

The root mean square value (RMS) of the random stress and strain for the given spectral density (see Figs. 8 and 9) can be obtained as follows :

The variance of the random stress

$$s_s^2=E\left[S^2\right] \qquad (30)$$

$$s_s^2=\frac{K^2}{A^2}E\left[y^2(t)\right] \qquad (31)$$

The standard deviation (RMS) of the stress is,

$$s_s=\frac{K}{A}E\left[y(t)\right] \qquad (32)$$

where A, k is the material geometrical.

Generalized Cumulative damage model

For general n-degree-of-freedom lumped parameter system with mass matrix $[m_i]$, stiffness matrix $[k_{ij}]$, damping matrix $[c_i]$, and column matrix of external random forces $[p_j]$, the total damage is the sum of that in each mode according to the linear damage criteria as follows :

$$E\left[\frac{da}{dN}\right]=E\left[\left(\frac{da}{dN}\right)_1\right]+E\left[\left(\frac{da}{dN}\right)_2\right]+E\left[\left(\frac{da}{dN}\right)_3\right]+---- \qquad (33)$$

and the standard deviation of stress is:

$$s_S=\frac{K}{A}E[y_i(t)]$$

where,

$$E[y_j(t)]=E[y_1(t)]+E[y_2(t)]+E[y_3(t)]+----- \qquad (34)$$

thus, the variance of response is

$$E[y_j^2(t)]=\sum_{i=1}^{m}\frac{Sp(w_i)w_i y_{ij}^2 y_{is}^2}{8x_i k_i^2} \qquad (35)$$

The symbols ψ_{ij} , ψ_{is} represent the eigen vectors for modal matrix of the structure [11], and s is the location where the random load is appled, ω_i is the eigenvalues of the structure which is different for various beams [12] (see appendix B).

It is possible to obtain multi shapes for the present generalized cumulative damage mode depending on the various RMS value and from equation (9) we obtain the following models .

$$E[\frac{da}{dN}]=\frac{fk}{mA}(2paD)^{1/2}[1-f(\frac{D-2x}{D})^n]^{1/2}\{\sum_{i=1}^{m}\frac{Sp(wi)wi\,y^{\,2}_{ij}y^{\,2}_{is}}{8xik_i^{\,2}}\}^{1/2} \qquad (36)$$

$$E[\frac{da}{dN}]=\frac{fk}{mA}(2paD)^{1/2}[1-f(\frac{D-2x}{D})^n]^{1/2}\{\sum_{i=1}^{m}\frac{Sp(wi)pf_i y^{\,2}_{ij}y^{\,2}_{is}}{4x_i k_i^{\,2}}\}^{1/2} \qquad (37)$$

$$E[\frac{da}{dN}]=\frac{fk}{mA}(2paD)^{1/2}[1-f(\frac{D-2x}{D})^n]^{1/2}\{\sum_{i=1}^{m}\frac{Sp(wi)p\,y^{\,2}_{ij}y^{\,2}_{is}}{4kici}\}^{1/2} \qquad (38)$$

$$E[\frac{da}{dN}]=\frac{fk}{mA}(2paD)^{1/2}[1-f(\frac{D-2x}{D})^n]^{1/2}\{\sum_{i=1}^{m}\frac{k_s^{\,2}(1+xi^2)Sp(wi)y^{\,2}_{ij}y^{\,2}_{is}}{4xiwi^3}\}^{1/2} \qquad (39)$$

Life prediction model

For the present work, the expected life prediction can be obtained from the previous cumulative damage models as follows:

$$E[N] = \int_{ai}^{ac} \frac{da}{\frac{fk}{mA}(2paD)^{1/2}\left[1 - f\left(\frac{D-2x}{D}\right)^{n}\right]^{1/2}\left\{\sum_{i=1}^{m} \frac{Sp(wi)wiy_{ij}^{2}y_{is}^{2}}{8xiki^{2}}\right\}^{1/2}} \quad (40)$$

$$E[N] = \int_{ai}^{ac} \frac{da}{\frac{fk}{mA}(2paD)^{1/2}\left[1 - f\left(\frac{D-2x}{D}\right)^{n}\right]^{1/2}\left\{\sum_{i=1}^{m} \frac{Sp(wi)pfiy_{ij}^{2}y_{is}^{2}}{4xiki^{2}}\right\}^{1/2}} \quad (41)$$

$$E[N] = \int_{ai}^{ac} \frac{da}{\frac{fk}{mA}(2paD)^{1/2}\left[1 - f\left(\frac{D-2x}{D}\right)^{n}\right]^{1/2}\left\{\sum_{i=1}^{m} \frac{Sp(wi)py_{ij}^{2}y_{is}^{2}}{2kici}\right\}^{1/2}} \quad (42)$$

$$E[N] = \int_{ai}^{ac} \frac{da}{\frac{fk}{\mu A}(2\pi 2\pi a)^{1/2}\left[1 - \varphi\left(\frac{D-2x}{D}\right)^{n}\right]^{1/2}\left\{\sum_{i=1}^{m} \frac{ks^{2}(1+\xi i^{2})Sp(\omega Sp(_{ij}^{2}\psi_{is}^{2}}{4\xi\xi i\omega^{3}}\right\}^{1/2}} \quad (43)$$

Discussion

Figs. (10) and (11) show the schematic representation of propagating and non-propagating cracks computed by the present model for 0.4% C steel and Al-2024 T_4 which are mounted as a simply-supported beams on the vibration exciter. The figures describe the effect of the function ϕ which depends on the crystallographic orientation of the neighboring grains, RMS values of the displacement and propagation and arrest of cracks. The figures indicate that, if the boundaries are impenetrable and the neighboring grain has zero RMS value of random stress and lighter damping, then the value of ϕ is unity and in this case the crack decelerates continuously until the crack becomes a non-propagating crack and arrest at grain boundary. The figures also show the case of long crack which occurs when the RMS values of stress of the two grains are equal (high stress) and then the value of ϕ is zero. The figures also indicate the cases of the propagation of cracks which occurs when the standard deviation of stress of neighboring grain is greater than the standard deviation of stress of the grain where the crack is initiated and this is the case of variability of the orientation ϕ from zero to unity.

Figs. (12-17) show the theoretical application of the model compared with the experimental results for the propagating and non-propagating selected cracks. The weakness of the barriers permit cracks to penetrable into the adjacent grains, the value of ϕ in this case varies from zero to unity ($0 < \phi < 1$) and represent the propagation of cracks which are initiated in the grain boundary and begins to decelerate when the propagation approaches the boundaries of the grain, but accelerate as the cracks propagate away from the boundary.

Figs. (18) and (19) show the variation in crack propagation rate with crack length where the parameter D (grain size) has to be considered and indicate the case of crack arrest and the ability of the cracks to overcome the stronger barrier .

Figures (20) and (21) show the propagation and non-propagation of cracks in beams of the two material mounted on the fixture as a cantilever where the mode shape gives the higher eigenvalues / vectors and standard deviation of stress and then the more rapid is the accumulation of damage.

For comparison between the two materials used in the present work, the previous figures indicate that the faster cumulative damage is in the 0.4% C steel and this is due to the higher stiffness, lighter damping, and the higher RMS value of the random stress compared with the second material.

The simulation of a structure is a powerful tool to understand the cumulative damage in different mode shapes.

The simulation proves the presented mathematical model in terms of more accurate model parameters and analyze the dynamic characteristics of the structure when it is subjected to random loading, study the initiation of cracks, Their propagation, and finally the failure of the structure taking into account the response vector (elements representing the response spectrum in each DOF), the excitation vector (elements representing the force spectrum in each DOF), degree of freedom (points & directions), frequency response matrix, and frequency response function.

Suspension : the structure bottom is fixed .

Analyzer : frequency rang 0-2000Hz $\Delta f = 3$Hz.

DOF's : typical DOF'S selected for the simulation as shown in Fig. (22)

Variable parameter : Excitation : random loading

Reference DOF :

1) oblique no.1

2) vertical no. 2

From the mode shapes, it can be seen that the higher modes show the largest rotations of the top plate, and hence the highest sensitivity for rotational inertia loading, However the structure is very light and the random loading problem will probably not exist for most practical structures.

When are analyzed the results presented in the simulation of the structure shown in Fig. (23), the following comments may be stated:

1. Case 1 represents the first mode natural frequency of the structure and first bending of vertical member. The natural frequency is 252 Hz. Case 1 uses the effect of the extreme stiffness and inertia ratios for the validation purpose.

2. Case 2 represents 2nd mode shape natural frequency which is the torsion of the vertical member.
3. The shear of vertical member is represented in case 3 which changes the stiffness characteristics of the system .
4. Cases 4, 5, 6 represent cases of torsion, transverse, and 1st and 2nd bending of top plate. For the 4th , 5th , and 6th modes, the dynamic response of the structure changes, as shifts in the eigen values, and eigen vectors.
5. The 2nd & 1st bending of top member is represented by the cases 7 and 8 which are the cases of the high natural frequencies, mode 7, 8 give indication for the variability of stiffness, damping, shifting of natural frequencies, or this is reflected in the spectrum of the response.
6. Case 9, mode 9 represents the case of initiation of cracks due to highest standard deviation of random stress of grain size of a point A.
7. Case 10 represents the case of the propagation of the crack tip into adjacent grains, there is migration of dislocations and there is localized plastic deformation.
8. Case 11 represents the case of the failure of the top plate due to an accumulation of damage model where the accumulated total damage reaches 100%.

From these concepts of design against cumulative damage and for any long-life fatigue for any material examined in the present model, one should optimize the structure or component by applying this model to obtain the curves of crack growth rate, propagating and non-propagating, variation in cracks, and the comparison of experimental and theoretical results. The model proposed here is based on certain assumptions regarding the actual conditions which are compared with experimental observations. The model is very flexible to analyze the spectral density of the applied random loading, the trajectories of slip bands, eigenvalues/vectors, and damping ratios.

The model is also capable of predicting the effect of the spectral density, geometry and material variability on the reliability of structural component subjected to random loading.

Understanding the influence of the important factors, such as load spectra, geometry, material will give a new insight to the problem of cumulative damage. The spectral density technique presented in this work is capable of including such factors.

The technique is useful to a designer since it allows him to interpret complex system in terms of frequency domain, mode shapes and damping ratios.

Conclusions

Theoretical and experimental results concerned with the demarcation of fatigue crack initiation and short crack propagation phases indicate that :

1. Crack propagation begins at a crack depth less than a grain diameter.
2. In the short fatigue crack region, the initial crack growth rate of small cracks is high but they decelerate as they approach the crystallographic barriers, depending on the random stress level, they are either arrested or only temporarily halted.
3. The crack growth rate is retarded as the crack approaches a grain boundary, but accelerates as the crack propagates away from the

boundary in the cases S_B/S_A is small but finite.

4. The long-life fatigue can be improved by :

a. reducing the standard deviation of the random stress by either strengthing the structure or increasing the damping in the relevant mode of vibration.

b. lowering the frequency of vibration by altering the structure's dynamic behaviour .

References

[1] De Los Rios E.R., Tang Z. and Miller K.J., Short crack Fatigue behaviour in a medium carbon steel, Fatgue Engng. Mater. Struct., Vol 7, No. 2, P97-108, (1984).

[2] DE LOS Rios , Mohamed H.J. and Miller K.J., A micro-mechanics analysis for short Fatgue crack growth, Fatgue and Fract. Engng. Mater., Vol 8 ,No. 1, P49-63, (1985).

[3] Ibrahim M.F. and Miller K.J., Determination of Fatgue crack initiation life, Fatgue of Eng. Material and structures , Vol 2, PP351-360 (1980) .

[4] Chan, K.S. and Lankford, J., A crack – tip strain model for the growth of small Fatgue cracks, scripta metallurgia, Vol 17, p 529, (1983).

[5] Mini Workshop, Fracture and interfaces. Com, Fatgue & Fracture . htm, P1-2, (1997).

[6] Charles, A., Statistical Engineering. Com , Fatgue & Fracture. htm , P1-2, (2001).

[7] Doeblin O., Measurement system, Tokyo, McGraw-Hill Inc., P174, (1975).

[8] Carl, C., Fatgue design, New jersy, USA, P56, (1982).

[9] Warburton G.B., The Dynamical behaviour of structure, 2nd Edn, oxford Pergmon press, P305-309, (1976).

[10] Crandall, H. and Mark D., Random vibration in mechanical system, New York, P112, (1963).

[11] Yuen M., A. numerical study of the eigen parameter of a damaged cantilevers, Sound and vibration J., Vol 3, P301-310, (1985).

[12] Bigges, J.M., Introduction to structural dynamic, N.Y., McGraw-Hill, (1964).

APPENDIX A

Fourier Transforms

For the response at location s for a force $f_j(t)$ applied at j is given by.

$$X_s(t)=\int_0^t f_j(t)h_{sj}(t-t)dt \qquad (A1)$$

Equation (A1) assumes that the excitation $f_j(t)$ commences at t=0 ; but for

$t > -\infty$ changing t to ∞ and τ to $\tau`$ where $\tau` = t-\tau$,

$$X_s(t) = \int_0^t f_j(t-t\ )h_{sj}(t\ `)dt\ ` \quad (A2)$$

$$X_s(w) = H_{sj}(w)Fj(w) \qquad (A3)$$

For excitation by the unit impulse $X_s(\omega)=Hs_j(\omega)$ and from the equation (A4)

$$X_s(t) = \frac{1}{2p}\int_{-\infty}^{\infty} F_j(w)Hsj(w)$$

$$\exp(\ iw\,t)\,dw \qquad (A4)$$

yield to

$$h_{s_j}(t) = \frac{1}{2p}\int_{-\infty}^{\infty} H_{s_j}(w)\exp(iwt)dw \quad (A5)$$

Thus the complex frequency response $Hs_j(\omega)$ is the Fourier transform of the unit impulse response $hs_j(t)$; hence

$$H_{s_j}(t) = \int_{-\infty}^{\infty} h_{s_j}(t)\exp(-iwt)dt \quad (A6)$$

APPENDIX B

Eigenvalues for Beam

For simply – supported beam

$$w_i = \frac{i^2 p^2}{L^2}(EI/m)^{1/2} \quad (B1)$$

Fixed – Hinged beam

$$w_i = \frac{(i+\frac{1}{4})^2}{L^2}(EI/m)^{1/2} \quad (B2)$$

Fixed – Fixed beam

$$w_i = \frac{(i+\frac{1}{2})^2 p^2}{L^2}(EI/m)^{1/2} \quad (B3)$$

Cantilever beam

$$w_i = \frac{(i-\frac{1}{2})^2 p^2}{L^2}(EI/m)^{1/2} \quad (B4)$$

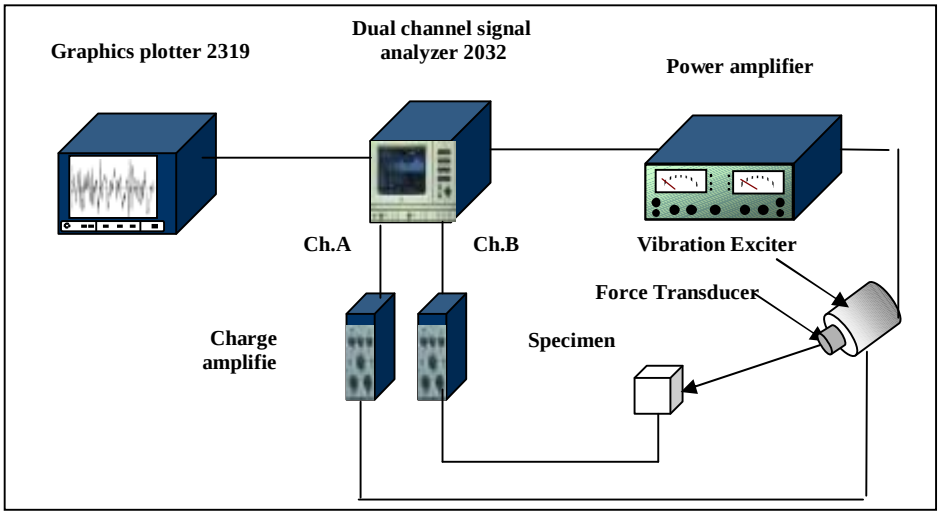

Fig. 1 Instruments used for the experiments

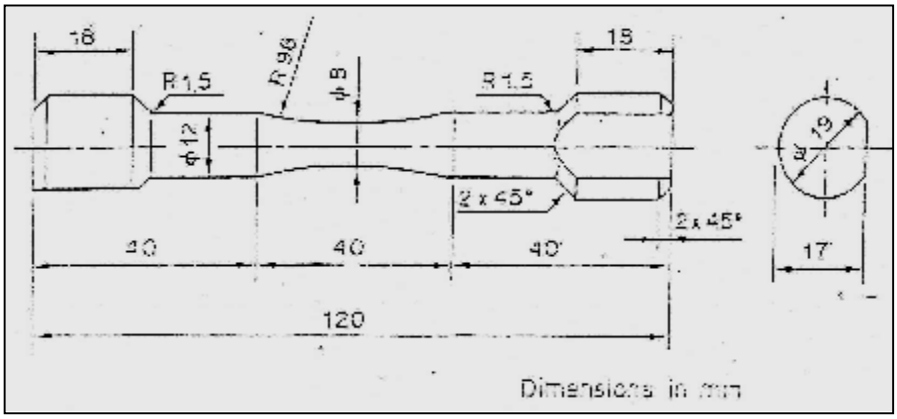

Fig. 2 Specimen geometry

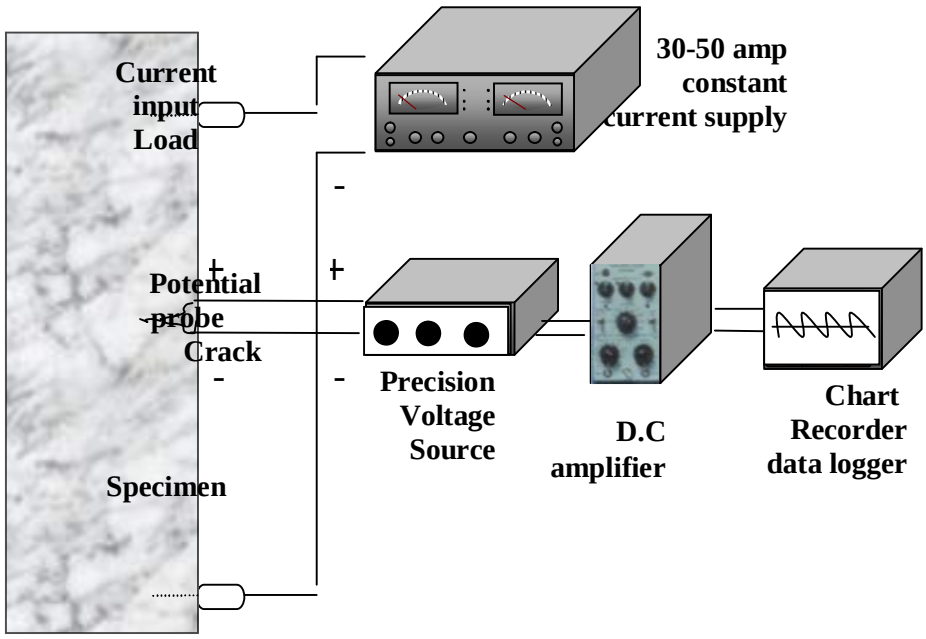

Fig.3 Block diagram of the D.C. Potential drop technique for crack length measurement

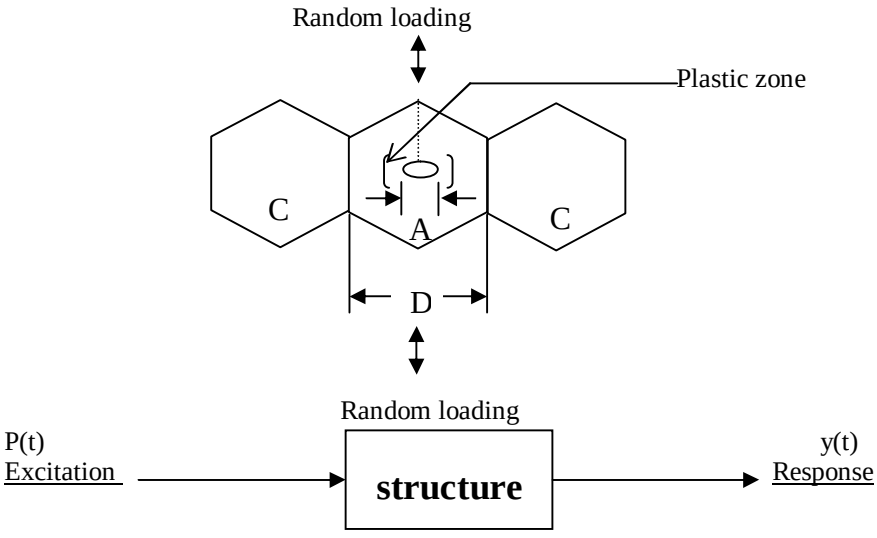

Fig. 4 Block diagram of excitation - response problem

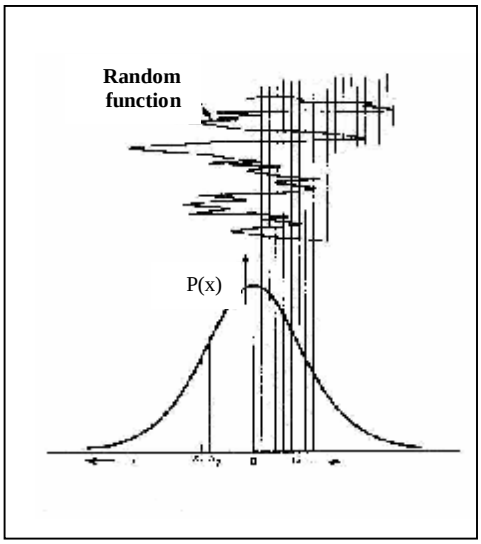

Fig. 5 Gaussian distribution of a random function [7]

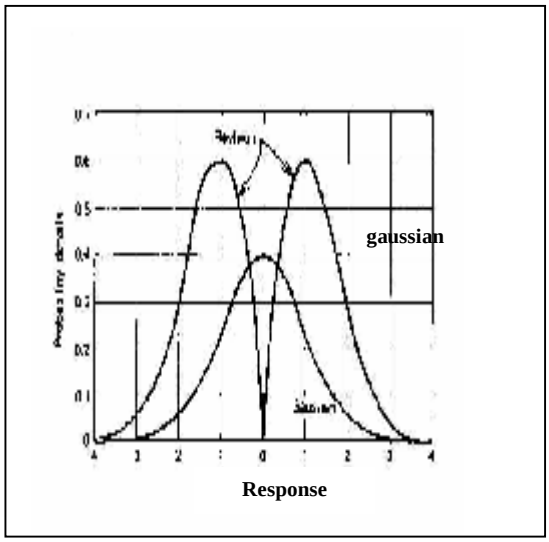

Fig. 6 Probability distributions. Rayleigh & Gaussian [7]

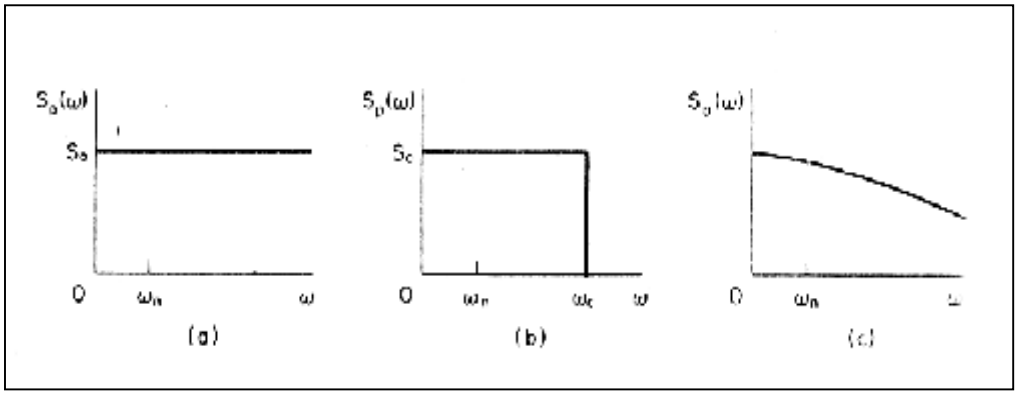

Fig. 7 Example of spectral density Sp(w) for an applied force

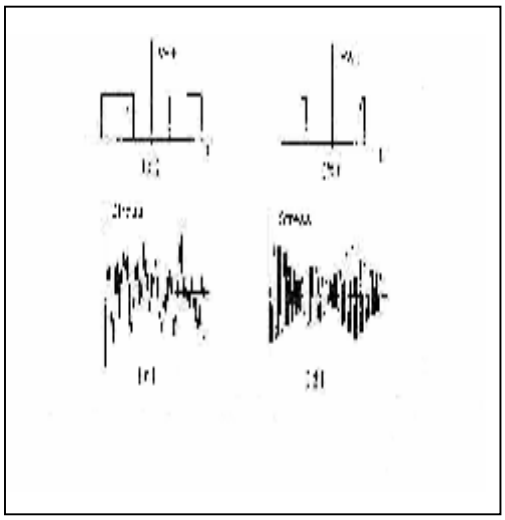

Fig. 8 Typical random loading and their power spectra
(a) & (c) broad band power spectrum and the corresponding loading . (b) & (d) narrow band power spectrum and the corresponding loading

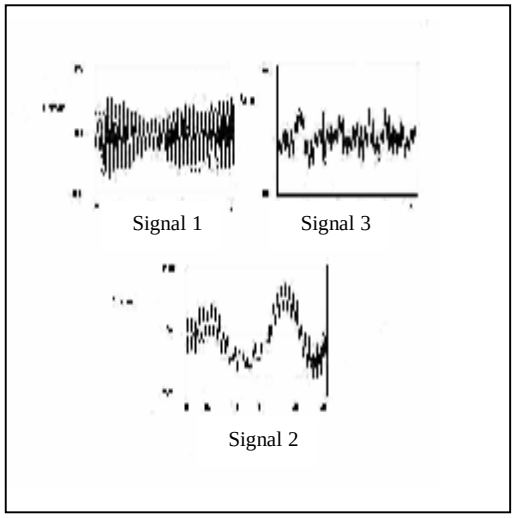

Fig. 9 Examples of random signals

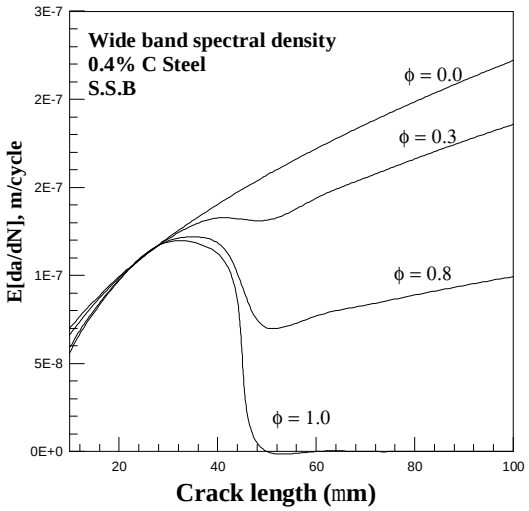

Fig. (10) Schematic representation of propagating and non-propagating cracks

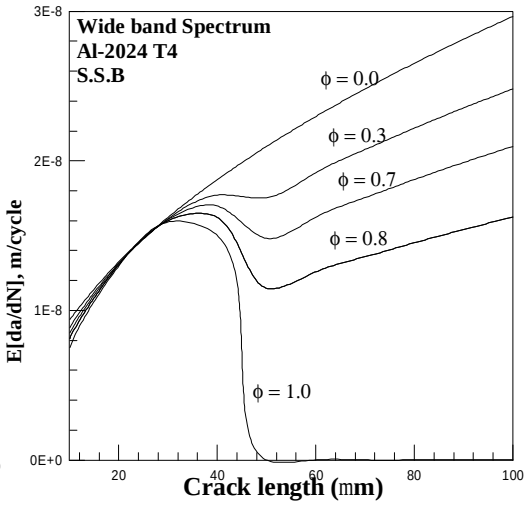

Fig.(11) Schematic representation of propagating and non-propagating cracks

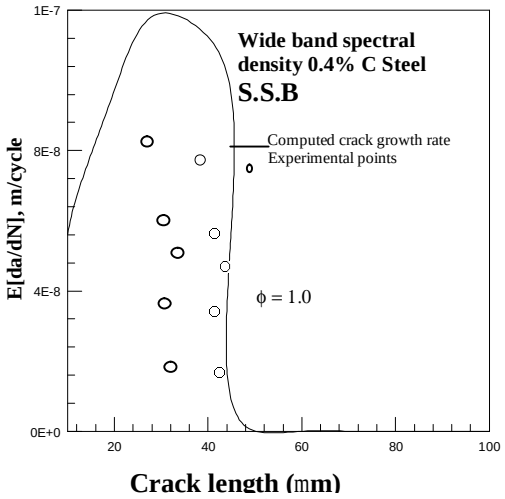

Fig. (12) Application of the model to selected crack

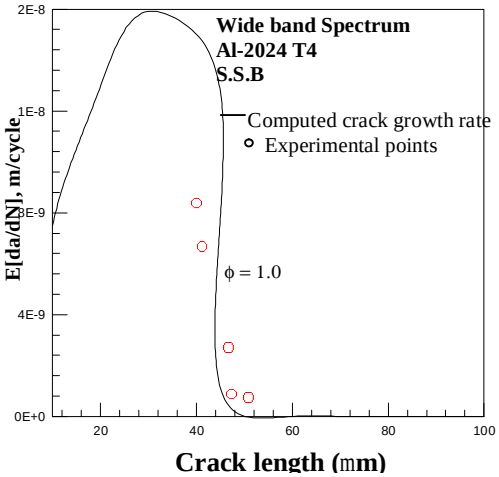

Fig. (13) Application of the model to selected crack

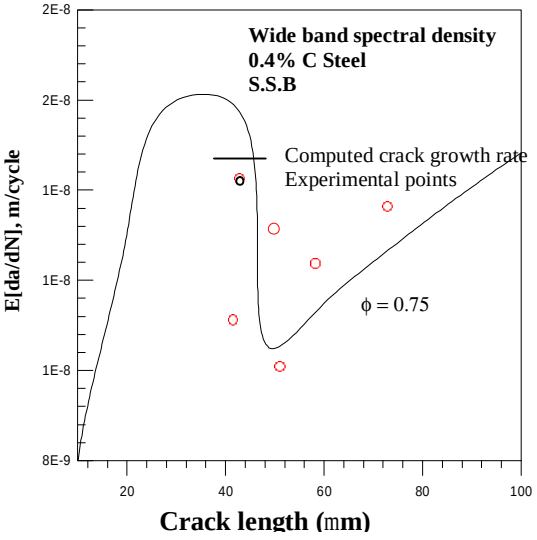

Fig. (14) Application of the model to selected crack

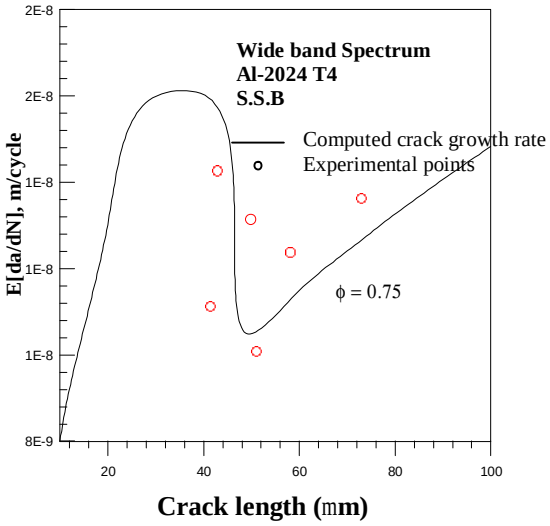

Fig. (15) Application of the model to selected crack

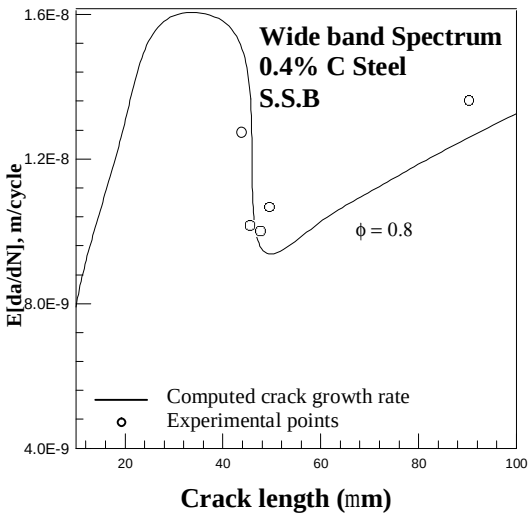

Fig. (16) Application of the model to selected crack

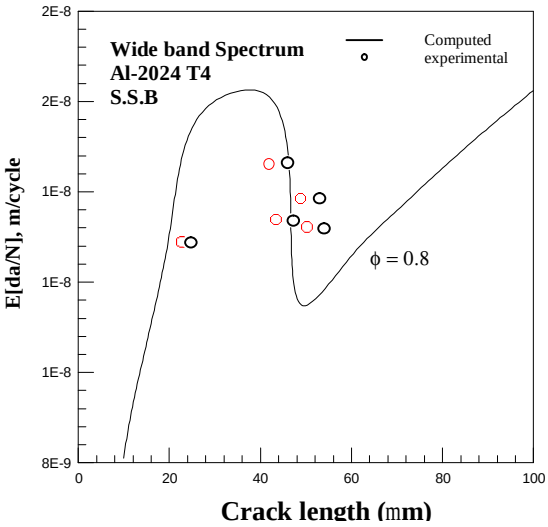

Fig. (17) Application of the model to selected crack

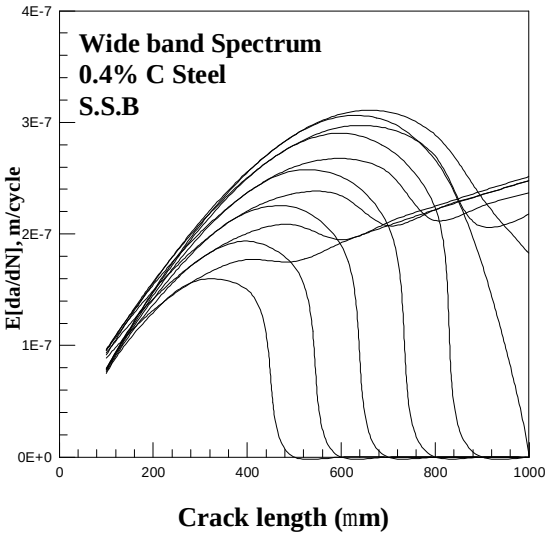

Fig(18) Variation of crack growth rate with crack length

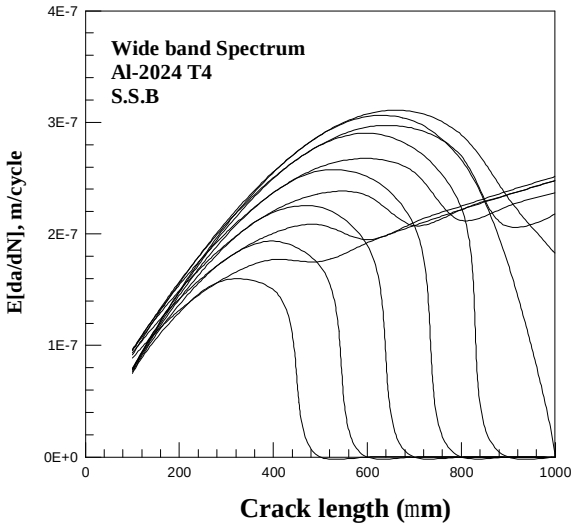

Fig. (19) Variation of crack growth rate with crack length

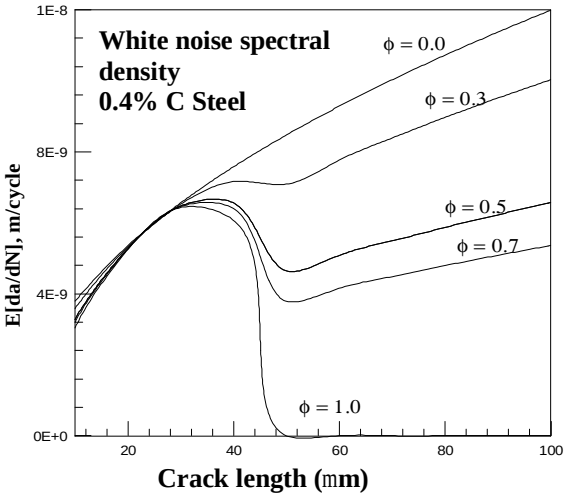

Fig. (20) Effect of eigenvalues/vectors on propagating and non-propagating cracks

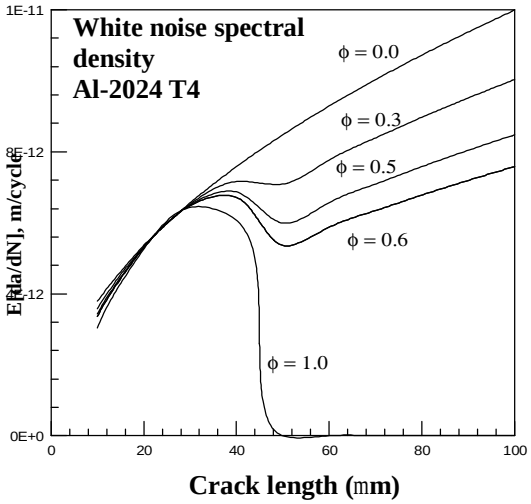

Fig. (21) Effect of eigenvalues/vectors on propagating and non-propagating cracks

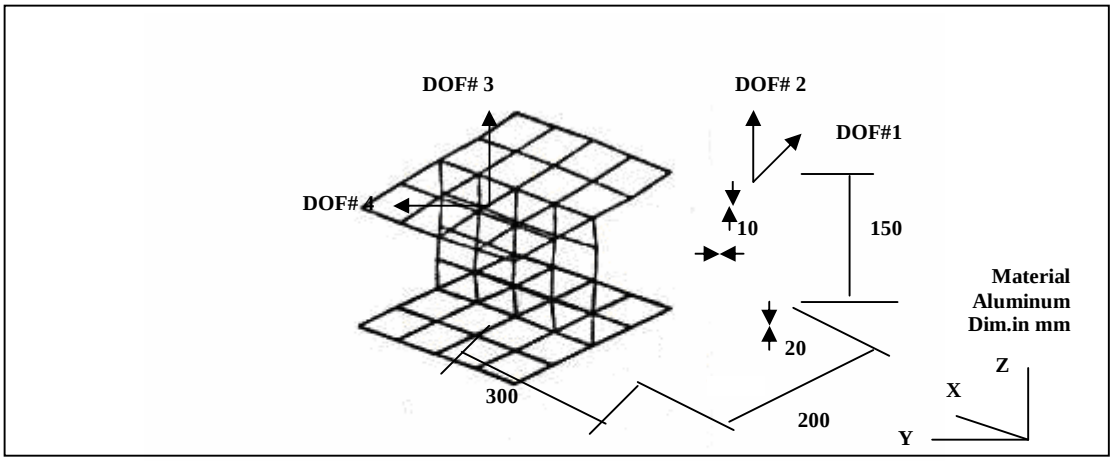

Fig. 22 Test structure

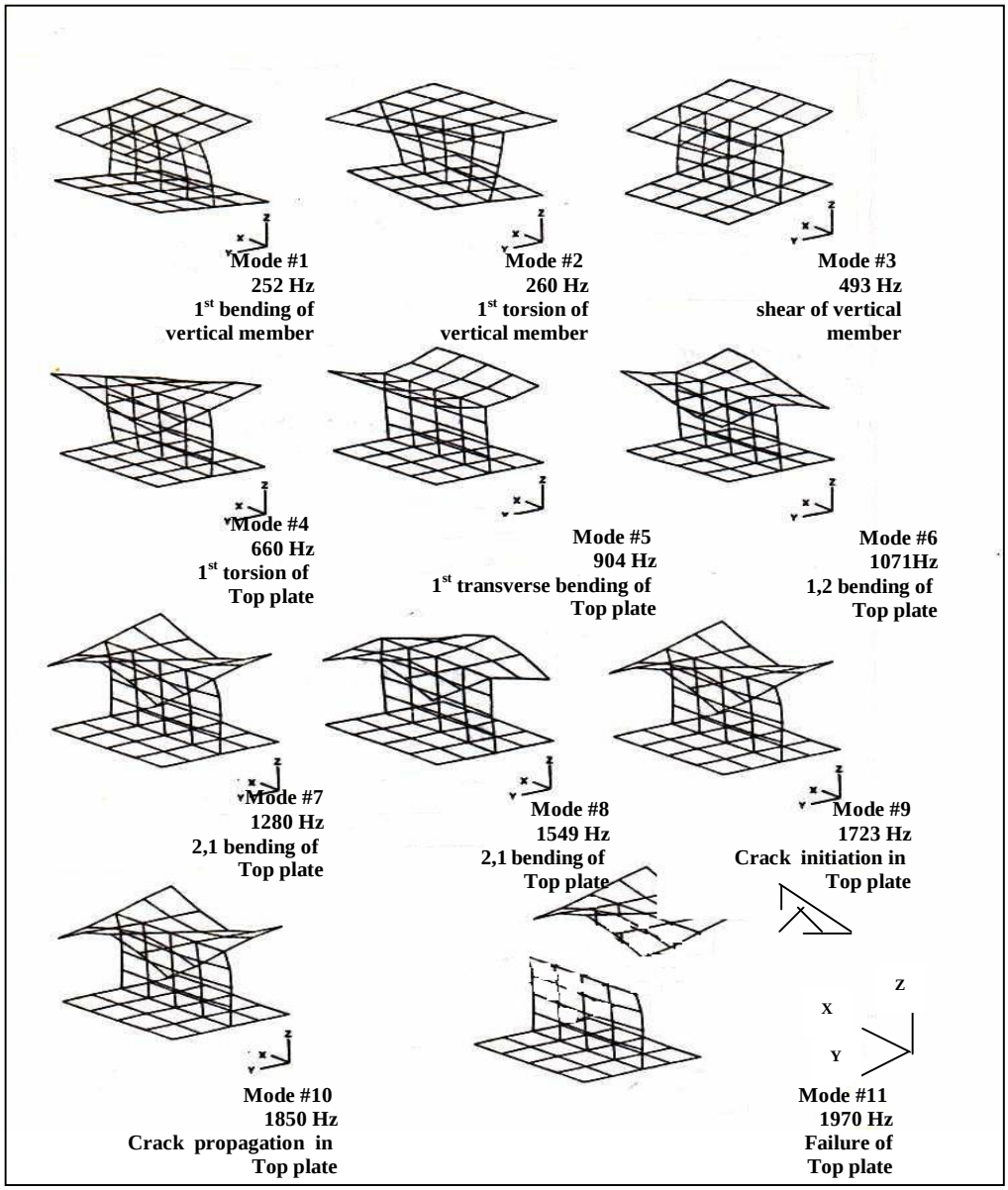

Fig. (23) Modal simulation of symmetrical structure